Supporting Information

A domino-like localized cascade toehold assembly amplification based DNA nanowire for microRNA imaging in living cell

Zizhong Yang,[a] Birong Liu,[a] Ting Huang,[a] Mengxu Sun,[a] Tong li,[a] Wen-Jun Duan,[a] Min-Min Li,[c] Jin-Xiang Chen, *[a] Zong Dai,[b] Jun Chen,*[a]

[a] NMPA Key Laboratory for Research and Evaluation of Drug Metabolism, Guangdong Provincial Key Laboratory of New Drug Screening, School of Pharmaceutical Sciences, Southern Medical University, Guangzhou, 510515, P.R. China

[b] Guangdong Provincial Key Laboratory of Sensing Techno logy and Biomedical Instrument, School of Biomedical Engineering, Sun Yat-Sen University, Shenzhen 518107, P.R. China

[c] Center of Clinical Laboratory, the First Affiliated Hospital of Jinan University, Guangzhou 510632, P.R. China.

E-mail: chenj258@smu.edu.cn

Table S1 Sequences of the Used Oligos

Description	Name	Sequences (5'-3')
	miR-221	AGCUACAUUGUCUGCUGGGUUUC
	miR-155	UUAAUGCUAAUUGUGAUAGGGGU
Assembly of LCTA for miR-221 analysis	H_1	TTCGCAAGCTACC**/iBHQ1dT/**CGAGCTACATTGTCTGCTGCCGCTCGAGATGGTAGCAGT
	S_1	GACGACTAATAAGATTAATCCTGTTTTGAAACCCAGCAGACAATGTAGCTCGA-**FAM**
	H_2	AGCTACATTGTCTTGCCTTCGCAAGCTACATGGTCGGAAGGCAGCTGGGTTTC
	S_2	TGTCCTAATTAGAATAATCTCGAGTTTACTGCTACCATGTAGCTTGCGAAGGC
Simultaneous detection of miR-221 and miR-155	H_{1a}	TTAATGCTAATTC**/iBHQ1dT/**CGAGCTACATTGTCTGCTGCCGCTCGAGGTGATAGGGGT
	S_{1a}	GACGACTAATAAGATTAATCCTGTTTTGAAACCCAGCAGACAATGTAGCTCGA-**FAM**
	H_{2a}	AGCTACATTGTCTTGCCTTAATGCTAATTGTGATCGTAAGGCAGCTGGGTTTC
	S_{2a}	TGTCCTAATTAGAATAATCTCGAGTTTACCCCTATCACAATTAGCATTAAGGC
L nanowires	L_1	ACAGGATTAATCTTATTAGTCGTCTCGTTACTTAAATGGTCAGAAATATGGGATTAACCATGGTGTTTATGATATGAAGTGTTGGAAGCT
	L_2	CTCGAGATTATTCTAATTAGGACATTAATCCCATATTTCTGACCATTTAACGAACGAAGCTTCCAACACTTCATATCATAAACACCATGG
Specificity investigation	Mis1	AGC UAC AUU GUC UGC UGG CUU UC
	Mis2	AGC UAC AUU CUC UGC UCG GUU UC
	MiR-1246	AAU GGA UUU UUG GAG CAG G
	MiR-222	AGC UAC AUC UGG CUA CUG GGU CUC
	MiR-373	GAA GUG CUU CGA UUU UGG GGU GU
	AS1411 aptamer probe	AATCCCATATTTCTGACCATTTAACGAACGATTGGTGGTGGTGGTTGTGGTGGTGGTGG
	anti-miR-221	GAAACCCAGCAGACAATGTAGCT

S1. Electrophoresis Verification of H_1L_1, H_2L_2 and L Nanowire Formation.

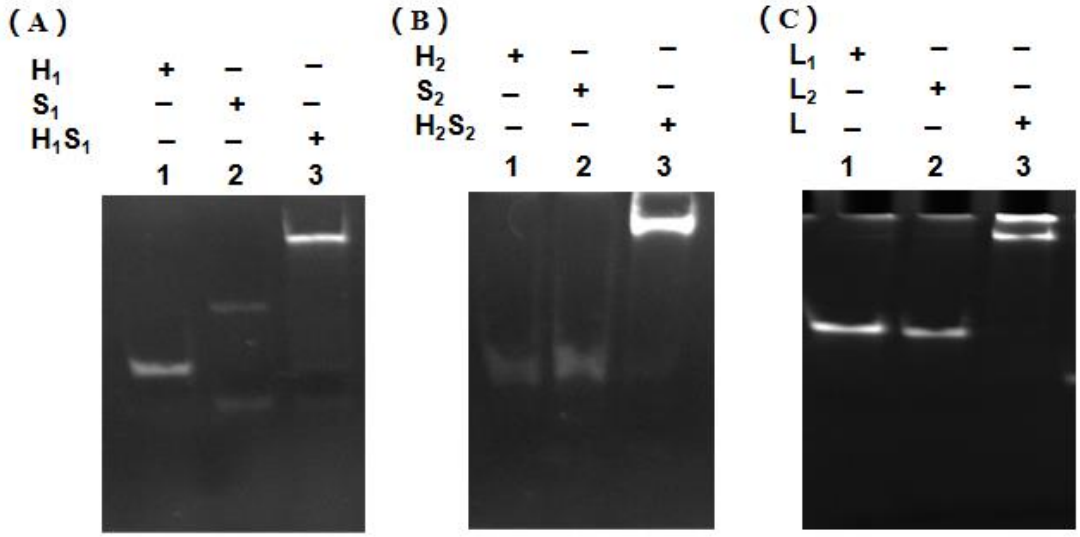

Figure S1. Electrophoresis Verification of H_1S_1, H_2S_2 and L Nanowire. (A) Lane 1: H_1; Lane 2: S_1, Lane 3: H_1S_1. (B)Lane 1: H_2, Lane 2: S_2, Lane 3: H_2S_2. (C)Lane1: L_1, Lane2: L_2, Lane 3: L Nanowire.

S2. Characterization of LCTA nanostructure by atomic force microscopy .

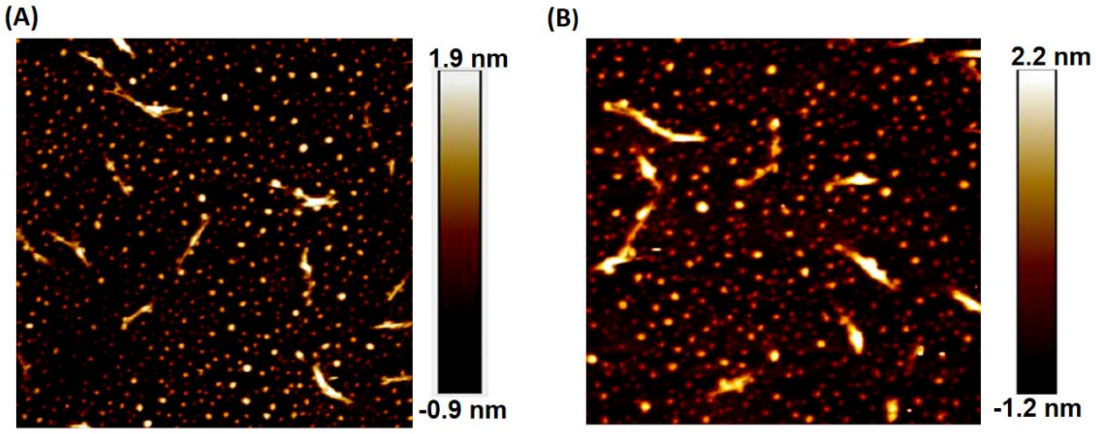

Figure S2. Atomic force microscopy imaging of L (A) and LCTA nanostructure (B).

S3. Thermodynamics calculation of the feasibility of CTA by NUPACK software.

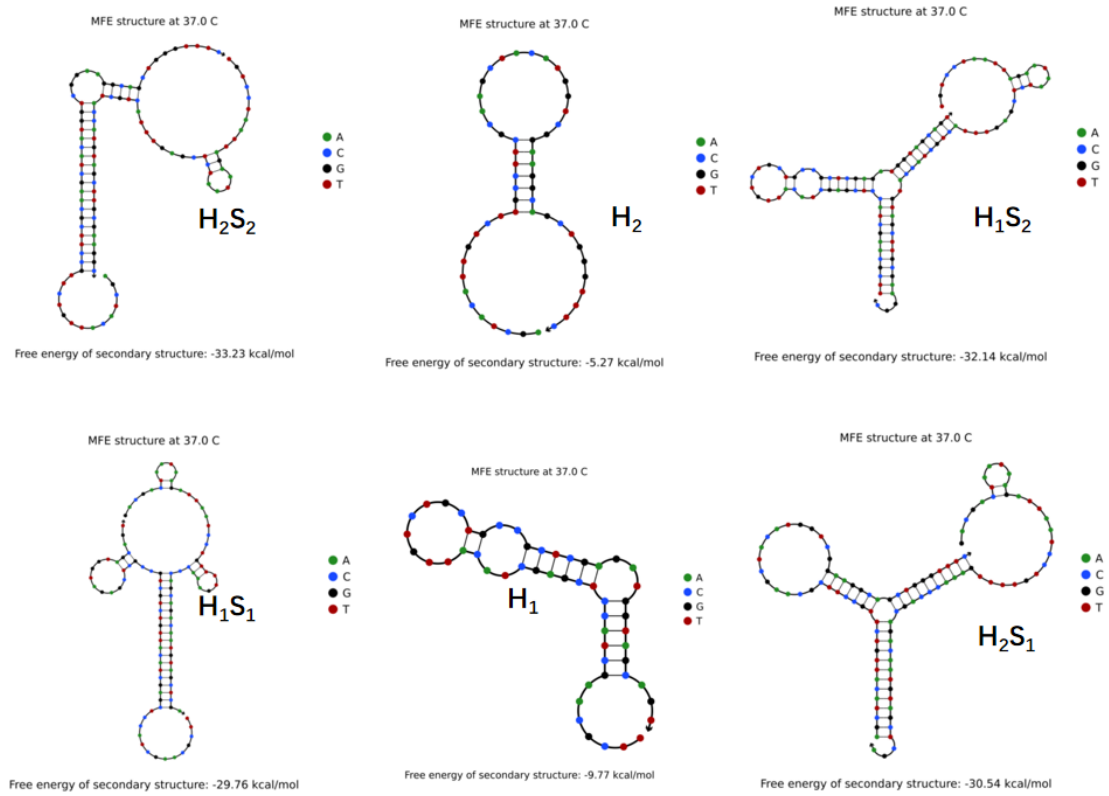

Figure S3. The free energy of different probes from NUPACK software.

In the LCTA strategy, a single strand trigger hybridized with S_2 is split into two segments and modified at both ends of the H_1. The H_1 in its hairpin state makes the two segments close to each other and acts as a single strand trigger to displace H_2 from H_2S_2. When H_1 reacts with H_2S_2 to release H_2, the released H_2 also has a tendency to self-fold into hairpin form, which can promote the hybridization of H_1 and S_2. For the reaction between H_1 and H_2S_2, H_1 can be treated as a single chain trigger with a ΔG nearly 0 kcal/mol to react with H_2S_2**.** When the ΔG of a reaction is less than zero ($\Delta G<0$), that means it can occur. The ΔG in the reaction between H_1 and H_2S_2 can be calculated by $\Delta G = \Delta G_{H1S2} + \Delta G_{H2} - \Delta G_{H2S2} + \Delta G_{Trigger}$. The ΔG of H_1S_2, H_2S_2 and H_2 are calculated as -32.14, -33.23 and -5.27 kcal/mol, respectively, which were obtained by NUPACK software (**Figure S3**). The ΔG is calculated to be -4.18 kcal/mol, indicating that H_1 can spontaneously react with H_2S_2 to replace H_2 in theory. Similarly, a miR-221 mimics was split into two segments and modified at both ends of the H2. The released H_2 from the H_2S_2 can further as a single chain miR-221 mimics target with the ΔG nearly 0 kcal/mol to react with H_1S_1**.** The ΔG of H_2S_1, H_1S_1 and H_1 are calculated as -30.54, -29.76 and -

9.77 kcal/mol, respectively (**Figure S3**). The ΔG in the reaction between H_2 and H_1S_1 can also be calculated by $\Delta G = \Delta G_{H2S1} + \Delta G_{H1} - \Delta G_{H1S1} - \Delta G_{target}$. The ΔG of the reaction between H_2 and H_1S_1 is calculated as -10.55 kcal/mol, which also indicates that H_2 can replace H_1 from H_1S_1. These results indicate that each step of the reaction in LCTA strategy is thermodynamically feasible.

.

S4. Analysis of the feasibility of LCTA system by PAGE electrophoresis.

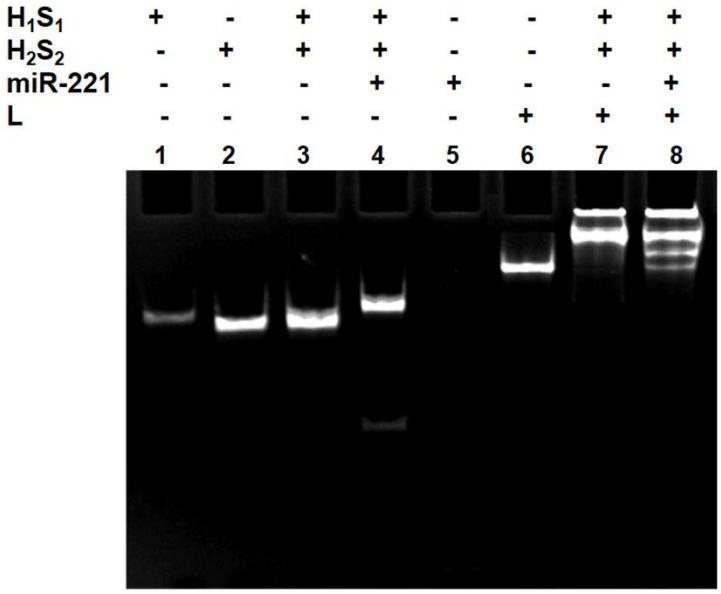

Figure S4. Electrophoresis characterization of the LCTA and CTA.

S5. Analysis of the Specificity of LCTA system.

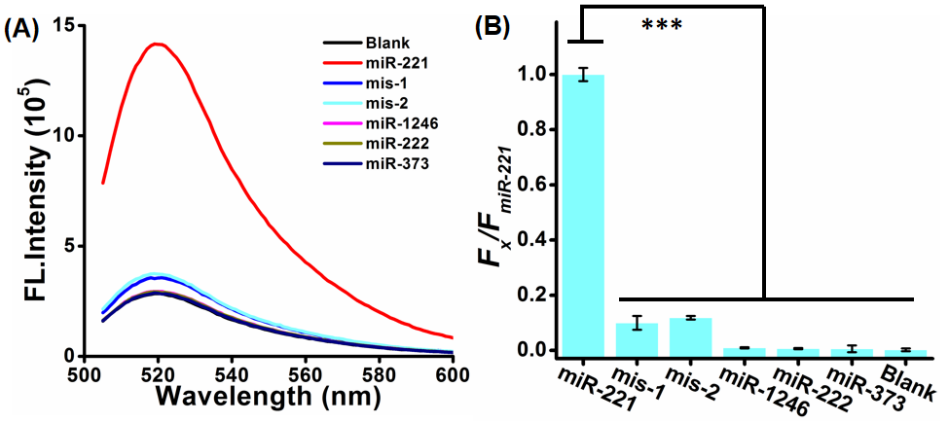

Figure S5. (A) Fluorescence spectra of LCTA containing 100 nM LCTA probes in response to the 100 nM miR-221 and other analogues at the same concentration. (B) Investigation of the specificity of the LCTA nanosystem upon the treatment with other analogues from miRNAs family. The data error bars indicate means ± SD (n=3, ***$p<0.001$).

S6. Nuclease-resistance of the LCTA.

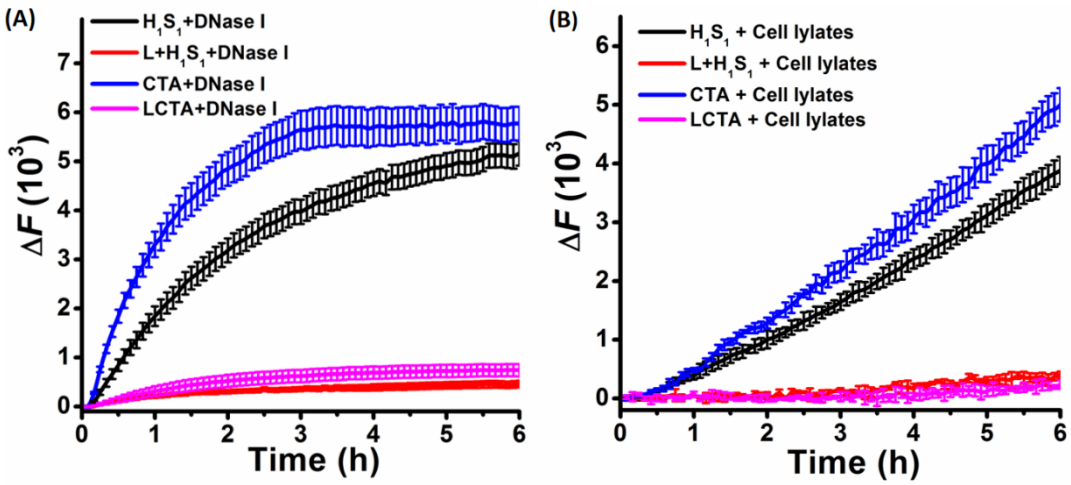

Figure S6. Stability of H_1S_1, CTA, L+H_1S_1 probe and LCTA in DNase I (A) and cell lylates (B). The data error bars indicate means ± SD (n=3).

S7. Cytotoxicity of the LCTA.

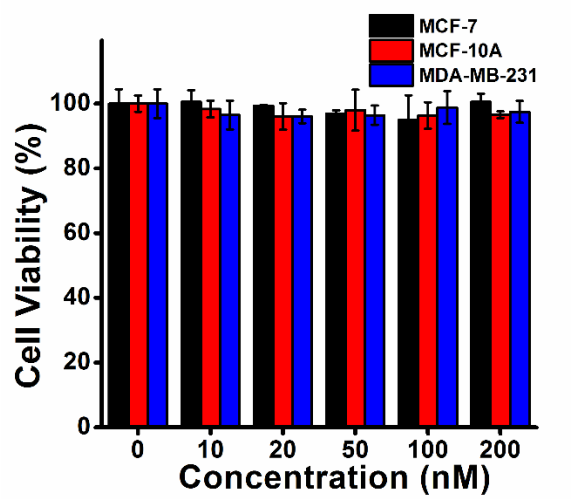

Figure S7. Cell viability of MCF-7, MCF-10A, and MDA-MB-231 cells after incubated with different concentrations of LCTA nanosystem for 24 h. Error bars represent the standard deviation of three replicates.

S8. CLSM images of MDA-MB-231 cells treated with different conditions.

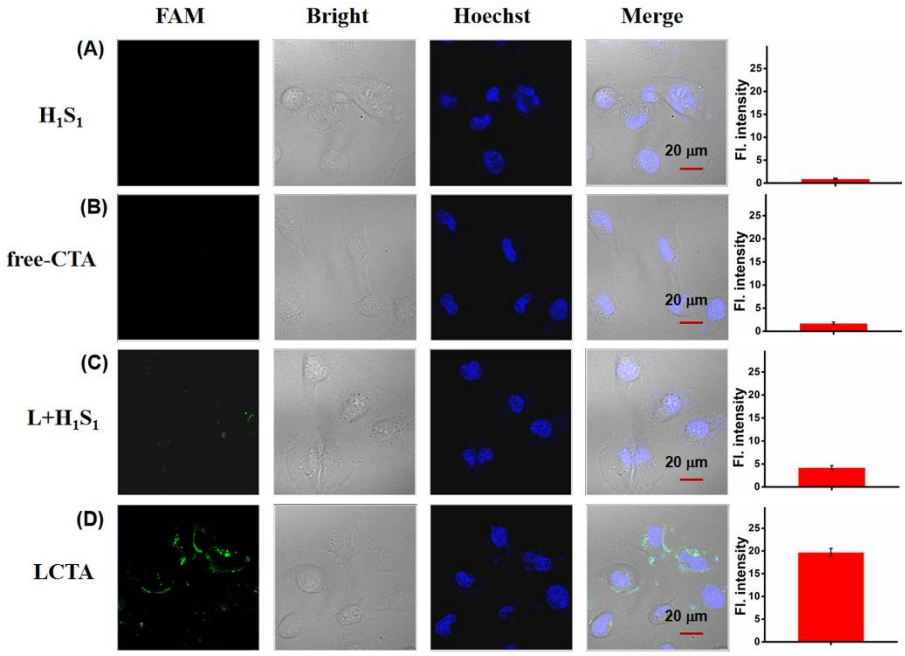

Figure S8. CLSM images of MDA-MB-231 cells treated with different conditions, from top to bottom: (A) H_1S_1 system, (B) CTA system, (C) L+H_1S_1 nanosystem and (D) LCTA nanosystem. Right, the mean fluorescence intensity of the cells in the FAM channel. Scale bar is 20 μm. The data error bars indicate mean ± SD (n = 3).

S9. Effects of dexamethasone on intracellular miR-221 imaging.

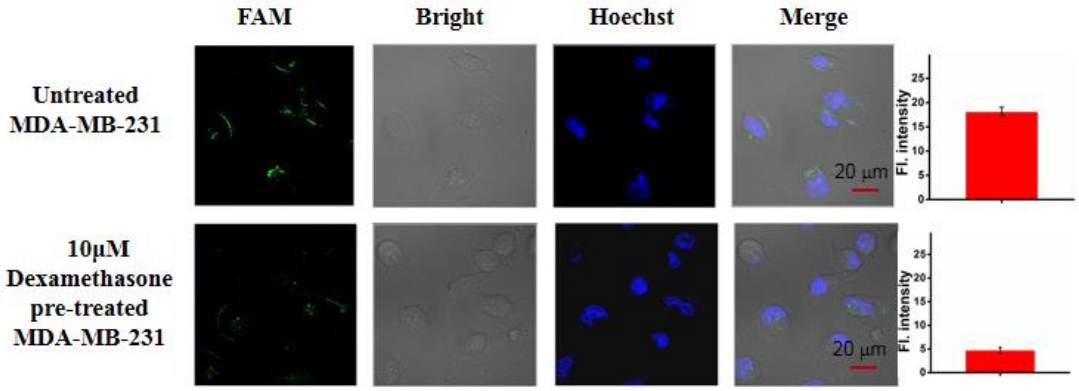

Figure S9. Untreated MDA-MB-231 cells, 10 μM dexamethasone pretreated MDA-MB-231 cells CLSM image after 3h incubation with nanosystem LCTA. Right, the mean fluorescence intensity of the cells in the FAM channel. Scale bar is 20 μm. The data error bars indicate mean ± SD (n = 3).

S10. Schematic of the OR gate logic sensor based LCTA system for miR-221 and miR-155 analysis.

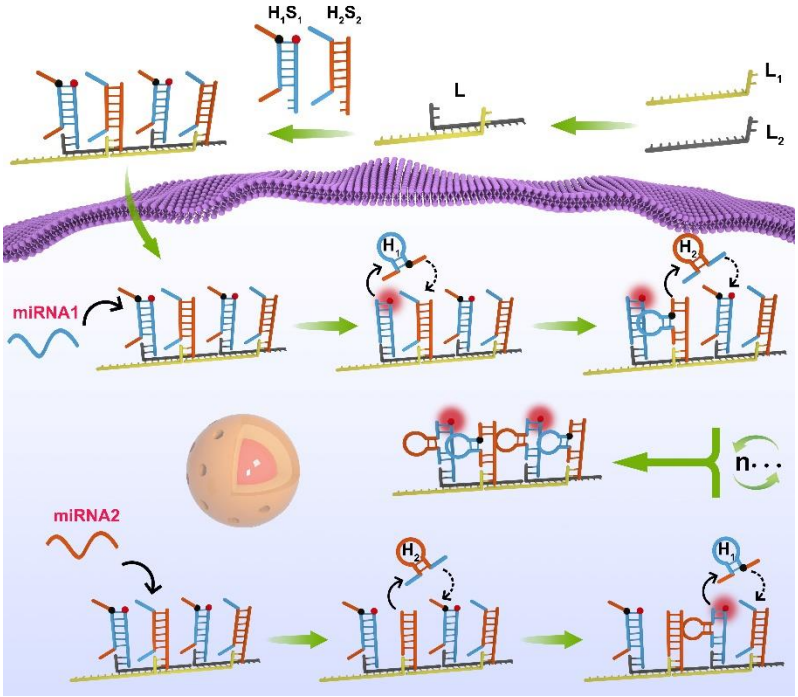

Figure S10. Schematic of the OR gate logic sensor based LCTA system for miR-221 and miR-155 analysis.

S11. Quantify the expression level of miR-221 by RT-qPCR.

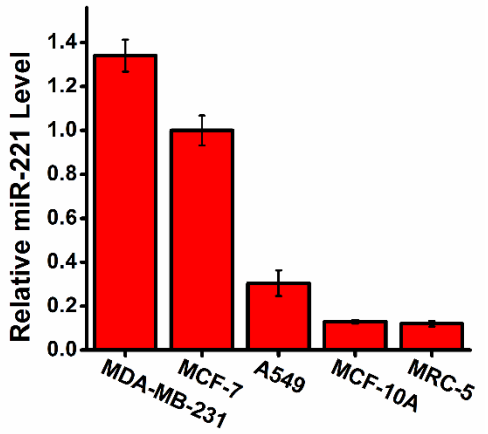

Figure S11. RT-qPCR analysis for the expression of the miR-221 in MDA-MB-231, A549, MCF-7, MCF-10A and MRC-5 cells. Error bars represent the standard deviation of three replicates.

S12. Quantify the expression level of miR-155 by RT-qPCR.

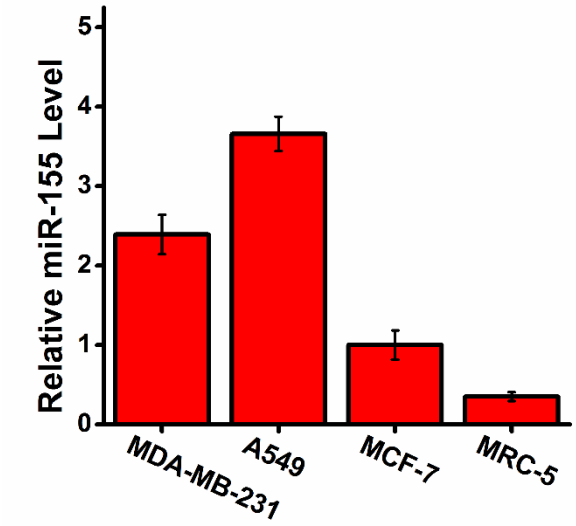

Figure S12. RT-qPCR analysis for the expression of the miR-155 in MDA-MB-231, A549, MCF-7 and MRC-5 cells. Error bars represent the standard deviation of three replicates.

S13. Effects of transfection reagents on intracellular miR-221 imaging in MCF-7 cell.

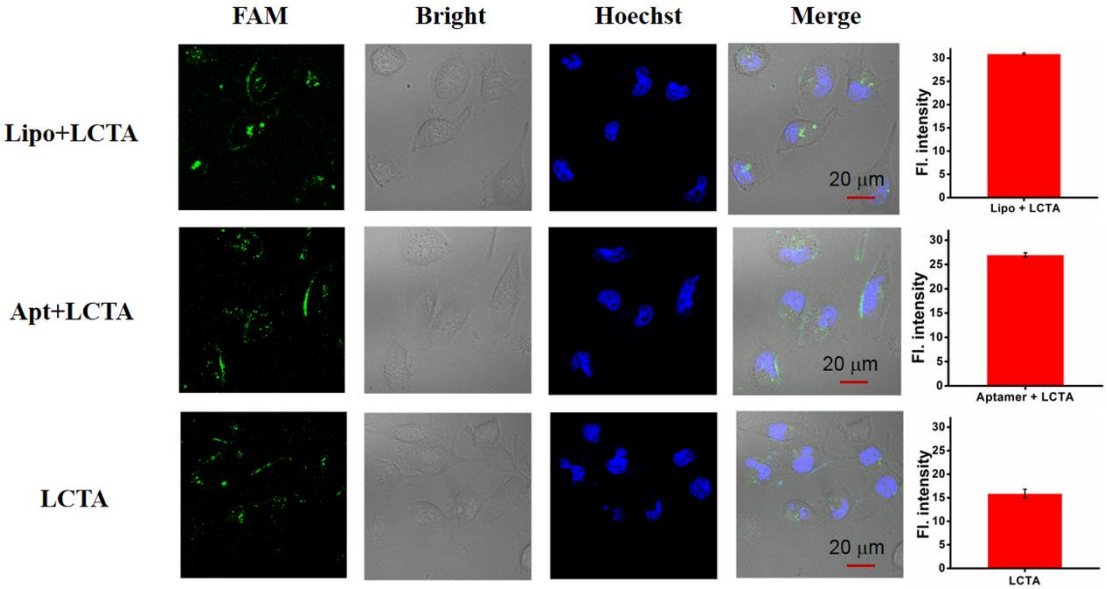

Figure S13. CLSM images of MCF-7 cells treated with different conditions, from top to bottom: (A) liposome 3000+LCTA, (B) Aptamer + LCTA, (C) LCTA nanosystem. Right, the mean fluorescence intensity of the cells in the FAM channel. Scale bar is 20 μm. The data error bars indicate mean ± SD (n = 3).